energies

MDPI

Article

CFD Simulation of Syngas Combustion in a Two-Pass Oxygen Transport Membrane Reactor for Fire Tube Boiler Application

Te Zhao [1], Chusheng Chen [2] and Hong Ye [1,*]

[1] Department of Thermal Science and Energy Engineering, University of Science and Technology of China, Hefei 230027, China; alamode@mail.ustc.edu.cn
[2] Collaborative Innovation Center of Chemistry for Energy Materials, Laboratory of Materials for Energy Conversion, Department of Materials Science and Engineering, University of Science and Technology of China, Hefei 230026, China; ccsm@ustc.edu.cn
* Correspondence: hye@ustc.edu.cn

Abstract: The oxygen transport membrane reactor technology enables the stable combustion of syngas and reduction in NO_x emission. Applying the syngas combustion membrane reactor to fire tube boiler can integrate oxygen separation, syngas combustion, and steam generation in a single apparatus. In this study, a CFD model for oxygen permeation and syngas combustion in a two-pass LSCoF-6428 tubular membrane reactor for fire tube boiler application was developed to study the effects of the inlet temperature, the sweep gas flow rate, and the syngas composition on the reactor performance. It is shown that the inlet temperature has a strong effect on the reactor performance. Increasing the inlet temperature can efficiently and significantly improve the oxygen permeability and the heat production capacity. A 34-times increase of oxygen permeation rate and a doubled thermal power output can be obtained when increasing the inlet temperature from 1073 to 1273 K. The membrane temperature, the oxygen permeation rate, and the thermal power output of the reactor all increase with the increase of sweep gas flow rate or H_2/CO mass ratio in syngas. The feasibility of the syngas combustion membrane reactor for fire tube boiler application was elucidated.

Keywords: oxygen transport membrane reactor; syngas combustion; fire tube boiler; CFD simulation; thermal power

check for updates

Citation: Zhao, T.; Chen, C.; Ye, H. CFD Simulation of Syngas Combustion in a Two-Pass Oxygen Transport Membrane Reactor for Fire Tube Boiler Application. *Energies* **2021**, *14*, 7348. https://doi.org/10.3390/en14217348

Academic Editors: Aiwu Fan and Guglielmo Lomonaco

Received: 8 September 2021
Accepted: 1 November 2021
Published: 4 November 2021

Publisher's Note: MDPI stays neutral with regard to jurisdictional claims in published maps and institutional affiliations.

Copyright: © 2021 by the authors. Licensee MDPI, Basel, Switzerland. This article is an open access article distributed under the terms and conditions of the Creative Commons Attribution (CC BY) license (https://creativecommons.org/licenses/by/4.0/).

1. Introduction

Coal, as one of the major fossil fuels, has been used to meet a very considerable fraction of the energy demands, and is likely to stay as a main energy source for mankind [1]. The utilization of coal results in the forming of pollutants such as SO_x, NO_x, greenhouse gas, and particulates. The development of efficient and clean coal utilization technology has become a top priority [2]. Coal gasification is currently one of the more mature clean coal technologies with coal as feedstock and air, CO_2, and H_2O as gasifying agent in a gasifier to produce gasified coal gas. The integration of coal gasification with the combined cycle plant (IGCC) is one of the most promising technologies for clean coal power generation, in which coal is first gasified under pressure to form a coal gas. After purification of the coal gas to remove ash, sulfide, and nitride, a relatively clean syngas is obtained, the main components of which are H_2 and CO. The syngas is then completely combusted in a gas turbine combustor. The exhausted gas is expanded in the turbine and then fed into a steam boiler to recover the waste heat [3]. However, it is worth noting that the syngas composition may vary widely, and this composition variability increases the difficulty of stable combustion and brings great challenges to the combustor design [4]. In addition, the syngas combustion in the gas turbine combustor will emit atmospheric pollutant NO_x, which needs to be controlled desperately.

The oxygen transport membrane reactor (OTMR) makes it possible to promote the stable combustion of syngas and the reduction in NO_x emission. The membrane, made of

ceramic materials that can transfer oxygen ions and electrons, is only permeable to O_2 while completely impermeable to other gases (such as N_2). Air can be separated to obtain 100% pure oxygen theoretically via the membrane. In this work, we first present the concept of the syngas combustion membrane reactor for application in a fire tube boiler. In an OTMR, air as the oxygen source is introduced to one side of the membrane, while syngas (H_2 + CO), the coal gasification product, is introduced into the other side. The syngas reacts with the permeated O_2 to generate CO_2 and H_2O and release a large amount of heat simultaneously. Because the membrane is completely permeable to oxygen, nitrogen, as well as $NO_{x,}$ would not appear in the product, therefore the costly subsequent purification process can be avoided. Furthermore, a high concentration of CO_2 can be captured after condensation of the product. Since the combustion of syngas releases a large amount of heat, the syngas combustion membrane reactor can be used as a fire tube in a fire tube boiler to heat the water outside the tube, which enables the integration of oxygen separation, syngas combustion, steam generation, and CO_2 capture in a compact apparatus. Recently, immense amounts of research have been conducted on the syngas production based on membrane reactor [5–9], while the research on the syngas combustion in an OTMR is still insufficient. MA. Habib et al. [10] developed a CFD model for syngas combustion in an OTMR and analyzed the change of oxygen permeability under the flow conditions with and without methane combustion, as well as the combustion characteristics of syngas. However, the heat production capacity of the membrane reactor is not clear. MA. Habib et al. [11] designed a methane combustion membrane reactor for fire tube boilers application and performed a numerical simulation analysis on a single membrane reactor. The results suggest that for a reactor unit with a length of 1.8 m, in order to meet the power demand of 5–8 MW, the final boiler system is 5 m high, and 12,500 membrane reactor units need to be installed. The total membrane area and total volume are 2700 m^2 and 45.45 m^3, respectively. R. Ben-Mansour et al. [12] designed a two-pass methane combustion membrane reactor applied to a fire tube boiler, and numerically investigated the combustion characteristics of CH_4 as well as the heat transfer characteristics of the reactor. IB. Mansir et al. [13,14] proposed a two-pass methane combustion reactor used in a fire tube boiler which can generate 1–5 MW power, and numerically investigated the effects of the emissivity and thermal conductivity of materials on the heat transfer behavior of the reactor.

In the present work, a concept of syngas combustion membrane reactor for fire tube boiler use was presented, $La_{0.6}Sr_{0.4}Co_{0.2}Fe_{0.8}O_{3-\delta}$ (LSCoF-6428) [10] was selected as the membrane material, and a steady-state CFD model for oxygen permeation and syngas combustion in a two-pass tubular membrane reactor for application in fire tube boilers was developed by using FLUENT software. The model was validated against the reported experimental data. Then, the effects of inlet temperature, the sweep gas flow rate, and the syngas composition on the membrane reactor performance, such as the membrane temperature distribution, the oxygen permeation rate, and, particularly, the heat production capacity of the reactor were thoroughly investigated.

2. Model

2.1. Descriptions of the Membrane Reactor

The application of syngas combustion in a two-pass oxygen transport membrane reactor is intended for use in a fire tube boiler, with a schematic diagram shown in Figure 1, where *x* represents the axial direction and *r* represents the radial direction. The reactor includes concentric parallel tubes with the inner tube made of LSCoF-6428 membrane, which separates the reactor into a feed side and a reaction side (or sweep side). The second tube, a baffle, is made of low thermal conductivity material. The outer shell tube made of quartz is in contact with external saturated water vapor. Air as oxygen source is fed into the feed side of the reactor. Syngas (CO + H_2) is in mixture with CO_2 as the sweep gas is fed into the sweep side, where CO_2 is used as a diluent. At elevated temperature, oxygen from the feed side transports through the membrane under the oxygen partial pressure difference and reacts with syngas in the reaction side to produce CO_2 and H_2O. The heat

produced by the combustion is transferred to the quartz tube via radiation and convection, which is used to heat the external water to generate high-temperature saturated steam.

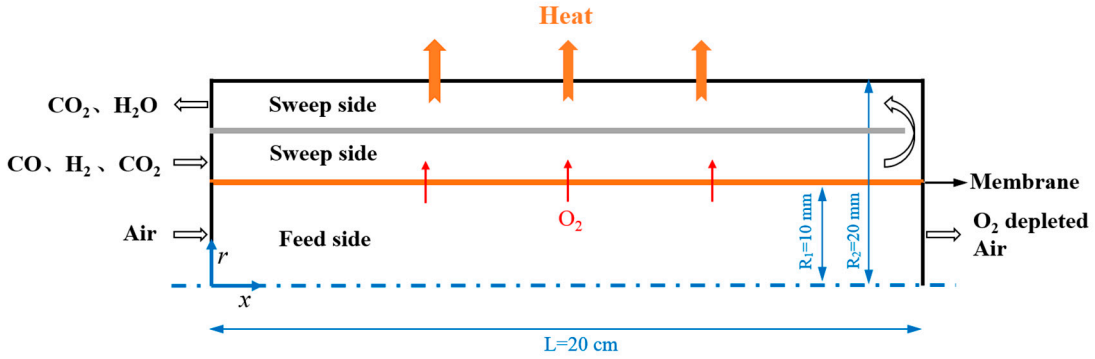


Figure 1. 2D axisymmetric representation of the syngas combustion membrane reactor.

2.2. Governing Equations

The operation of the membrane reactor is assumed to be at steady state with laminar flow in both feed and reaction sides. The outer quartz tube of the reactor is assumed to be isothermal and impermeable. The permeation of oxygen through the OTM is achieved by sink and source terms. In the regions adjacent to the membrane, oxygen is permitted to disappear from the feed side through the sink term and to appear on the sweep side through the source term [10]. The heat conduction process of the membrane is also taken into consideration, and the chemical reaction only occurs in the reaction side. The mathematic model describing the processes of flow, heat, and mass transfer, as well as reaction for the two-dimensional axisymmetric (x- and r-coordinates) reactor geometry, includes the following governing conservation equations [15].

Continuity equation:

$$\frac{\partial}{\partial x}(\rho u) + \frac{1}{r}\frac{\partial}{\partial r}(r\rho v) = S_i \quad (1)$$

Momentum conservation equations:

x-momentum equation:

$$\frac{\partial}{\partial x}(\rho uu) + \frac{1}{r}\frac{\partial}{\partial r}(r\rho vu) = -\frac{\partial p}{\partial x} + \frac{\partial}{\partial x}\left(\mu\frac{\partial u}{\partial x}\right) + \frac{1}{r}\frac{\partial}{\partial r}\left(r\mu\frac{\partial u}{\partial r}\right) \quad (2)$$

r-momentum equation:

$$\frac{\partial}{\partial x}(\rho uv) + \frac{1}{r}\frac{\partial}{\partial r}(r\rho vv) = -\frac{\partial p}{\partial r} + \frac{\partial}{\partial x}\left(\mu\frac{\partial v}{\partial x}\right) + \frac{1}{r}\frac{\partial}{\partial r}\left(r\mu\frac{\partial v}{\partial r}\right) - \mu\frac{v}{r^2} \quad (3)$$

Energy conservation equation:

$$\frac{\partial}{\partial x}\left(\rho c_p uT\right) + \frac{1}{r}\frac{\partial}{\partial r}\left(r\rho c_p vT\right) = \frac{\partial}{\partial x}\left(k\frac{\partial T}{\partial x}\right) + \frac{1}{r}\frac{\partial}{\partial r}\left(rk\frac{\partial T}{\partial r}\right) + S_h \quad (4)$$

Species balance equation:

$$\frac{\partial}{\partial x}(\rho uY_i) + \frac{1}{r}\frac{\partial}{\partial r}(r\rho vY_i) = \frac{\partial}{\partial x}\left(\rho D_{i,m}\frac{\partial Y_i}{\partial x}\right) + \frac{1}{r}\frac{\partial}{\partial r}\left(r\rho D_{i,m}\frac{\partial Y_i}{\partial r}\right) + S_i + R_i \quad (5)$$

where u and v are the gases velocity components in the x- and r-directions, respectively, p is the local pressure, T is the local temperature, ρ is the fluid density, μ is the fluid dynamic viscosity, k is the effective thermal conductivity, S_h is the energy source term due to chemical reaction, R_i is the species i production rate due to chemical reaction, and calculation of R_i requires a chemical kinetic mechanism discussed below, and Y_i is the mass fraction of

species i. The diffusion coefficient $D_{i,m}$ is calculated based on the binary mass diffusion coefficient of the component i in the component j [16]:

$$D_{i,m} = \frac{1 - X_i}{\sum_{j,j \neq i} \left(\frac{X_i}{D_{i,j}} \right)} \tag{6}$$

where X_i is the mole fraction of species i, and $D_{i,j}$ is binary mass diffusion coefficient calculated by using the Chapman–Enskog equation based on the kinetic theory [17].

S_i is the mass source or sink term (kg/m^{3}s) accounting for the species permeation across the membrane [10]. As the membrane is only permeable to O_2, the source/sink term is zero unless $i = O_2$, as shown in the following expression:

$$S_i = \begin{cases} +\frac{J_{O_2} A_{cell} MW_{O_2}}{V_{cell}}, & \text{at reaction side} \\ -\frac{J_{O_2} A_{cell} MW_{O_2}}{V_{cell}}, & \text{at feed side} \end{cases} \tag{7}$$

where J_{O_2} is the oxygen permeability of the OTM (mol/m^2·s), and calculation of J_{O_2} is discussed below, A_{cell} and V_{cell} are the cells' area (m^2) and volume (m^3), respectively, and MW_{O_2} is the oxygen molecular weight (kg/mol). S_i is positive in the sweep side and negative at the feed side.

Xu and Thomson [18] proposed an explicit oxygen permeation model for the membranes such as LSCoF-6428, combining surface exchange on the feed and sweep sides and bulk diffusion in terms of the oxygen partial pressures. The parameters determined by Xu and Thomson only apply to the membranes without chemical reactions. Rui et al. [19] modified this oxygen permeation model by adding a factor α to the model; taking the reducing atmosphere at the reaction side into account, the modified model is shown as follows:

$$J_{O_2} = \frac{\left(\frac{\alpha k_{r1}}{k_{f1}} \right) P_2^{-0.5} - \left(\frac{\alpha k_{r2}}{k_{f2}} \right) P_1^{-0.5}}{\frac{1}{k'_{ex}} + \frac{2\delta}{D_V} + \frac{1}{k''_{ex}}} \tag{8}$$

where P_1 and P_2 are the oxygen partial pressures in the feed and sweep side, respectively, δ is the membrane thickness, and k_f, k_r and D_V are the forward and reverse surface exchange rate constant and the oxygen vacancy bulk diffusion coefficient, respectively. In the present study, α takes the same value, of 1.65, as that by Rui et al. [19]. $k'_{ex} = k_{f2} P_1^{0.5}$ and $k''_{ex} = k_{f1} P_2^{0.5}$ are the surface exchange coefficients of the membrane referring to the feed and reaction sides, respectively. The expressions of k_f, k_r, and D_V are as follows, where T_1 and T_2 are the temperatures of membrane surface referring to the feed and reaction sides, respectively, T_{ave} is the average temperature, and $T_{ave} = (T_1 + T_2)/2$:

$$\begin{cases} k_{f1} = 5.89 \times 10^4 \exp(-27{,}300/T_1) \\ k_{f2} = 5.89 \times 10^4 \exp(-27{,}300/T_2) \end{cases} \left(\text{m/atm}^{0.5}\text{s} \right) \tag{9}$$

$$\begin{cases} k_{r1} = 2.07 \times 10^8 \exp(-29{,}000/T_1) \\ k_{r2} = 2.07 \times 10^8 \exp(-29{,}000/T_2) \end{cases} \left(\text{mol/m}^2\text{s} \right) \tag{10}$$

$$D_V = 1.58 \times 10^{-6} \exp(-8851.7/T_{ave}) \left(\text{m}^2/\text{s} \right) \tag{11}$$

In this work, the discrete ordinates (DO) model is used to calculate the radiative transfer equation (RTE) for simulating the solid and gas radiation heat transfer. The RTE in the direction $\vec{s}$ is provided as follows:

$$\frac{dI\left(\vec{r}, \vec{s}\right)}{ds} + (a + \sigma_s) I\left(\vec{r}, \vec{s}\right) = an^2 \frac{\sigma T^4}{\pi} + \frac{\sigma_s}{4\pi} \int_0^{4\pi} I\left(\vec{r}, \vec{s}'\right) \Phi\left(\vec{s}, \vec{s}'\right) d\Omega' \tag{12}$$

where I is radiation intensity, and r and s are position and path length, respectively. a and σ_s are absorption and scattering coefficients, respectively. n is the refractive index. Weighted sum of gray gases model (WSGGM) is used to calculate the absorption coefficient of the gases.

The laminar finite-rate model is used to calculate the POM reaction. The reaction rates calculated from Arrhenius rate expressions appear as the source term in the species balance equation of the laminar finite-rate model. In this simulation, the chemical kinetic equations of the syngas combustion are given as follows [20]:

$$CO + 0.5O_2 \rightarrow CO_2 \quad (13)$$

$$R_1 = 2.30 \times 10^{11} \exp\left(-\frac{31{,}700}{RT}\right)[CO][H_2O] \quad (14)$$

$$CO_2 \rightarrow CO + 0.5O_2 \quad (15)$$

$$R_2 = 4.45 \times 10^{9} \exp\left(-\frac{41{,}300}{RT}\right)[CO_2] \quad (16)$$

$$H_2 + 0.5O_2 \rightarrow H_2O \quad (17)$$

$$R_3 = 1.35 \times 10^{8} \exp\left(-\frac{6900}{RT}\right)[H_2]^{0.87}[O_2]^{1.1} \quad (18)$$

where R_i (i = 1,2,3) is the reaction rate.

2.3. Geometry and Boundary Conditions

The internal radii of the quartz tube, the baffle, and the membrane tube are set as 20, 15, and 10 mm, respectively. The membrane thickness is 1 mm. The baffle is 19.5 cm long and the tube length is 20 cm. The density of the membrane is 6000 kg/m^3. The thermal conductivity of the membrane is 4 W/(m·K). The emissivity of the membrane and the quartz tube are set to be 0.8 [21]. The thermal conductivity of the baffle is 0.1 W/(m·K), and the emissivity of the baffle is assumed to be 0.95. The composition, dimension, and physical parameters of the membrane reactor are summarized in Table 1.

Table 1. Composition, dimension, and physical parameters of membrane reactor.

Oxygen Transport Membrane	**$La_{0.6}Sr_{0.4}Co_{0.2}Fe_{0.8}O_{3-\delta}$ (LSCoF-6428)**
Effective length of membrane reactor	20 cm
Effective length of baffle	19.5 cm
Internal radii of quartz tube	20 mm
Internal radii of baffle	15 mm
Internal radii of membrane tube	10 mm
Thickness of baffle	1 mm
Thickness of membrane	1 mm
Density of membrane	6000 kg/m^3
Thermal conductivity of membrane	4 W/(m·K)
Emissivity of membrane and quartz tube	0.8
Thermal conductivity of baffle	0.1 W/(m·K)
Emissivity of baffle	0.95

The geometry is divided into two flow domains; one is the feed zone and the other is the sweep zone. The two domains are separated by a membrane wall. The mass flow inlet conditions are defined at the inlet boundary of feed and reaction side, while the pressure outlet conditions are adopted at the outlet of the two sides. Air (79% and 21% by moles of N_2 and O_2) is supplied into the feed side with a fixed mass flow rate of 6×10^{-4} kg/s. Syngas ($CO + H_2$) in mixture with CO_2 is supplied into the sweep side with a fixed 0.4/0.6

mass ratio of (CO + H_2)/CO_2. The quartz tube is assumed to be isothermal, and the temperature of the quartz tube wall is set to the saturation temperature of steam at 20 bar, which is 485 K. The pressures of the inlet gas streams are assumed to be 1 atm for both sides. Table 2 gives the variation range of boundary condition parameters in the subsequent parametric studies.

Table 2. Variation range of boundary condition parameters in parametric studies.

Inlet Temperature of Two Sides (K)	Mass Flow Rate of Sweep Gas (kg/s)	H_2/CO Mass Ratio
1073	2×10^{-6}	0.1:0.9
1123	6×10^{-6}	0.3:0.7
1173	1×10^{-5}	0.5:0.5
1223	2×10^{-5}	0.7:0.3
1273	4×10^{-5}	0.9:0.1

The effect of change in the inlet temperature of two sides is investigated while keeping the mass flow rate of sweep gas at 6×10^{-5} kg/s and the H_2/CO mass ratio at 0.5/0.5. Similarly, the effect of the sweep gas mass flow rate is investigated while keeping the two sides inlet temperature at 1173 K and the H_2/CO mass ratio at 0.5/0.5. Last, the effect of the H_2/CO mass ratio is analyzed while keeping the two sides' inlet temperature at 1173 K and the sweep gas mass flow rate at 6×10^{-5} kg/s. The inlet temperature of 1173 K, the sweep gas flow rate of 6×10^{-5} kg/s, and the H_2/CO mass ratio of 0.5/0.5 are the base case values.

2.4. Solution Procedures

The commercial CFD software FLUENT is used for the combustion modeling. Due to the axial symmetry property of the reactor, the geometry is simulated as a 2D axisymmetric unit. The segregated solver is used for solving the governing equations. Steady state is assumed. Laminar flow is considered due to the low flow rates. The energy model is adopted to solve the energy equation. The discrete ordinate model is considered for the radiation of the species. The incompressible ideal gas assumption is made for all the gases. The laminar finite-rate chemical kinetics model is adopted to simulate the chemical reactions. The SIMPLE pressure–velocity coupling scheme is adopted. The second-order upwind discretization scheme is chosen for pressure, momentum, energy, species, and the discrete ordinate. The convergence criteria for all the species, continuity, momentum, and energy residuals are set as 10^{-9}.

Two numerical models are used in this work. The first model is the oxygen permeation model through the OTM using the set of oxygen permeation Equations (8)–(11). These equations are defined in the FLUENT via a series of user-defined functions (UDFs) written in C++ language; the code is then compiled and hooked to FLUENT software. Three macros are used in the UDF for oxygen permeation model: The "Define Initialize", "Define Adjust", and "Define Source". They are considered for adding and subtracting the source/sink term in continuity and species transport equations. The second model in the present work is the chemical kinetics model of syngas combustion (Equations (13)–(18)), which can be simulated by using the laminar finite-rate model in the FLUENT. In order to guarantee the accuracy of the numerical simulation, grid independence test is performed. Finally, the structured grid with a grid number of 77,600 is used for calculation. In addition, the numerical model is validated with the reported experimental data in the literature as presented in the next section.

3. Validation of the Model

Due to the lack of experimental data for the syngas combustion in the OTMR, the oxygen permeation model and the syngas combustion kinetic model are validated independently.

3.1. Validation of Oxygen Permeation Model

The oxygen permeation model developed for the syngas combustion in the LSCoF-6428 membrane reactor is validated by comparison with the experimental data from Jin et al. [22,23]. The experiment was conducted in a tubular LSCoF-6428 membrane reactor with dimensions of 16 and 5 mm in internal diameters of quartz tube and membrane tube, 1.73 cm in length, and 1.5 mm in membrane thickness. The membrane separates the reactor into a shell side and a tube side. Air (100 cm^3(STP)/min) was fed into the shell side, while pure helium (62 cm^3(STP)/min) was introduced into the tube side. The operating pressure was 1 atm and the operating temperature was changed in the range of 1098–1173 K. The same conditions are modeled in the present validation work. Because the sweep gas used in this validation is helium, i.e., there is no reaction in this side, the value of α in Equation (8) is assumed to be 1 in this model validation work. As shown in Figure 2, the simulation result is in good agreement with the experimental data, reflecting the reliability of the oxygen permeation model for the simulation with helium as the sweep gas in the membrane reactor. When the syngas is used as the sweep gas, the value of α is taken as 1.65, according to the research of Rui et al. [19].

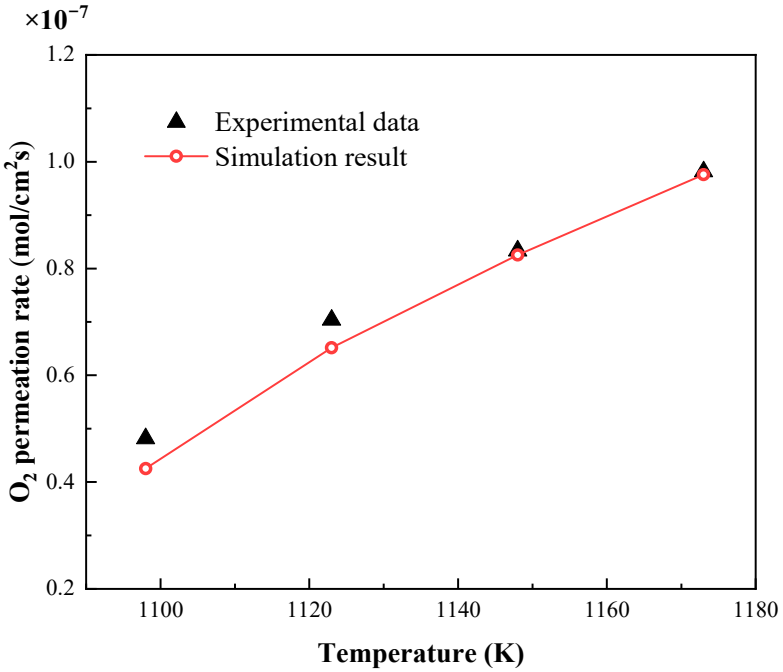


Figure 2. Comparison of O_2 permeation rate between simulation result and experimental data.

3.2. Validation of Syngas Combustion Kinetic Model

The syngas combustion kinetic model is validated against the experimental data of Barlow et al. [24]. The experiments were carried out on $CO/H_2/N_2$ jet flames. A tubular combustor with 196 mm diameter and 400 mm length was used. The nozzle was placed in the center of the entrance with 4.58 mm diameter. The fuel (40% CO, 30% H_2, and 30% N_2) jets into the combustor from the nozzle, and there is an air flow around the jet. The jet flow of fuel is provided at a velocity of 76 m/s and an inlet temperature of 292 K. The air flow around the jet is provided at a velocity of 0.75 m/s and an inlet temperature of 290 K. The pressure of fuel and air are kept at 1 atm. The temperature of the combustor external wall is fixed at 300 K. Due to the turbulent jet combustion occurring in the reactor, the RNG k-e model is used to solve the flow and the EDC model is used to simulate the combustion reaction. The comparison of simulation results and experimental data of syngas combustion is shown in Figure 3, where the mass fraction of CO and H_2 are taken from the center line of the reactor along the axis. It can be seen that the concentrations of CO and H_2 gradually decrease along the axis, and the syngas is consumed at a position of

approximately 0.2 m. The simulation results are in good agreement with the experimental data, indicating that the kinetic model is appropriate for the simulation of the syngas combustion process in the oxygen transport membrane reactor.

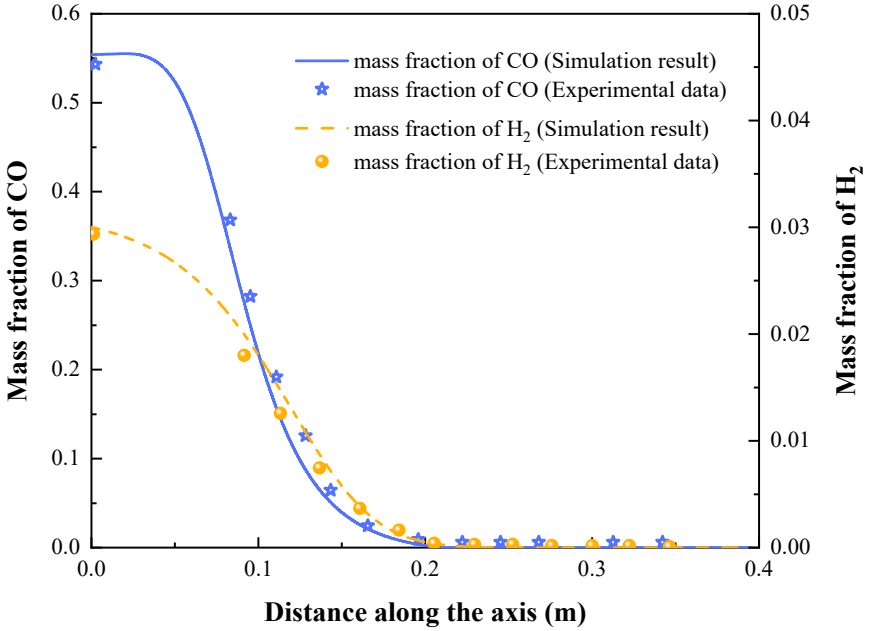


Figure 3. Comparison between simulation results and experimental data in terms of mass fractions of CO and H_2.

4. Results and Discussion

4.1. Effects of Inlet Temperature

Some operation parameters are known to have influence on the combustion characteristics of the OTMR, such as the inlet temperature, the sweep gas flow rate, and the fuel composition (i.e., syngas composition). In order to fully understand the effects of these parameters on the performance of the membrane reactor, parametric studies are carried out. In this section, the effects of inlet gas temperature are investigated by varying the temperature from 1073 to 1273 K. The other parameters are fixed at the base case values described in Section 2.3.

Figure 4 shows the effect of inlet gas temperature on the membrane temperature. There is radiative heat transfer between the membrane and the outer baffle and quartz tube near the exit, and there is convective as well as radiative heat transfer between the membrane and the gases on both sides of the reactor. It can be seen that the maximum temperature of the membrane appears at the inlet of the reactor and decreases gradually along the axis, mainly due to the heat exchange with the outer low-temperature baffle and rises slightly due to the flexural flow near the exit, then drops at the exit due to the radiative heat transfer with the outermost low-temperature quartz tube. The membrane temperature increases with the increase of the inlet gas temperature on both sides.

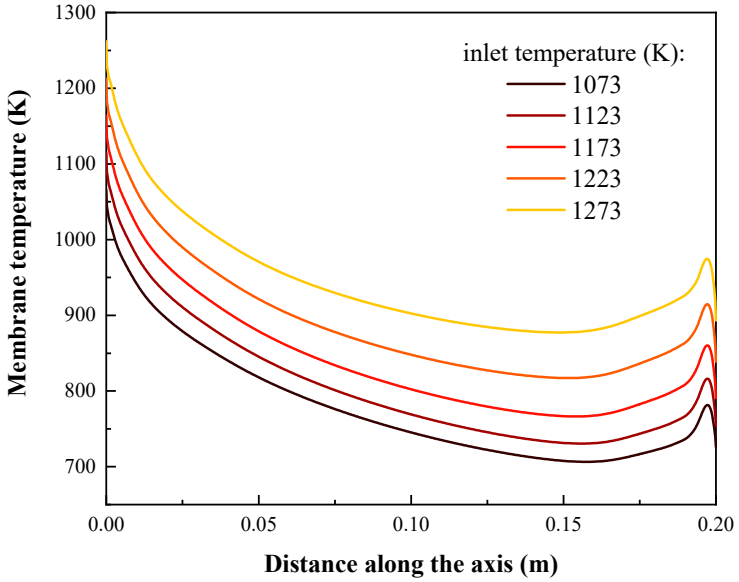


Figure 4. Effect of inlet temperature on membrane temperature distribution.

Figure 5 presents the effect of inlet gas temperature on the oxygen permeation rate across the OTM. Obviously, the inlet temperature has a significant effect on the oxygen permeation, and the oxygen permeation rate increases drastically with the increase of inlet temperature. When the inlet gases are supplied at temperature from 1073 to 1173 K, the averaged oxygen permeation rate along the axis increases from 0.59×10^{-7} to 5.04×10^{-7} mol/cm^2·s, which increases by more than seven times. When the inlet temperature rises to 1273 K, the averaged oxygen permeation rate increases to 20.46 mol/cm^2·s, which is about 34 times that at 1073 K. Therefore, higher temperature is required for proper functioning of the membrane to support the syngas combustion with sufficient oxygen.

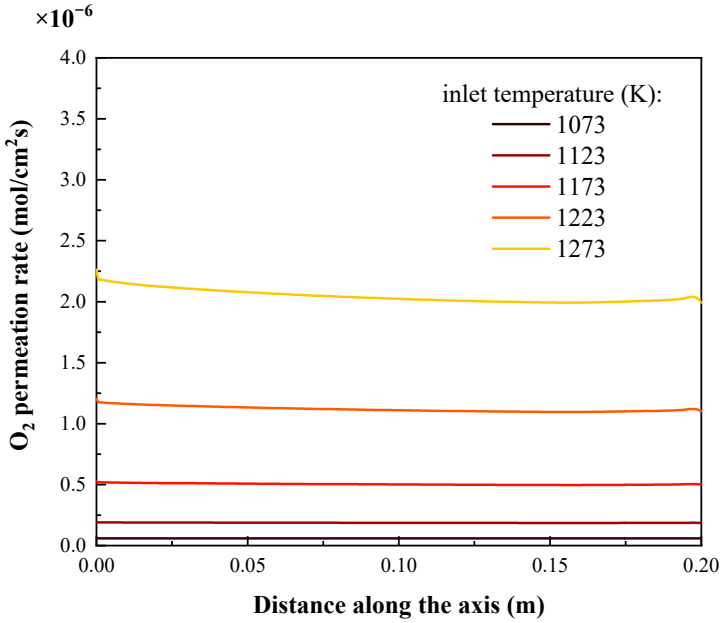


Figure 5. Effect of inlet temperature on oxygen permeation rate.

Figure 6 gives the effect of inlet gas temperature on the heat transfer rate to the outermost quartz tube (the load), i.e., the thermal power of the membrane reactor. It includes both the radiation and convection components to evaluate the total heat transfer rate to the load. As shown in Figure 6, the total heat transfer rate is found to increase

with increase of the inlet temperature. When the inlet temperature varies from 1073 to 1273 K, the radiative heat transfer accounts for approximately 72–78% of the total heat transferred to the load, while the convection component is approximately 22–28%. As the inlet temperature increases, the radiative heat transfer rate increases rapidly while the convective heat transfer rate increases relatively slowly. Therefore, the proportion of radiative heat transfer gradually increases while the proportion of convective heat transfer gradually decreases. The total heat transfer rate at 1073 K is 188.89 W, and the power density (i.e., the heat transfer rate per unit area of membrane) is approximately 15 kW/m^2. When the inlet temperature rises to 1273 K, the total heat transfer rate increases to 383.81 W, about twice that at 1073 K. The inlet temperature has a strong effect on the thermal power of the reactor. Increasing the inlet temperature can efficiently and significantly improve the heat production capacity of the syngas combustion membrane reactor.

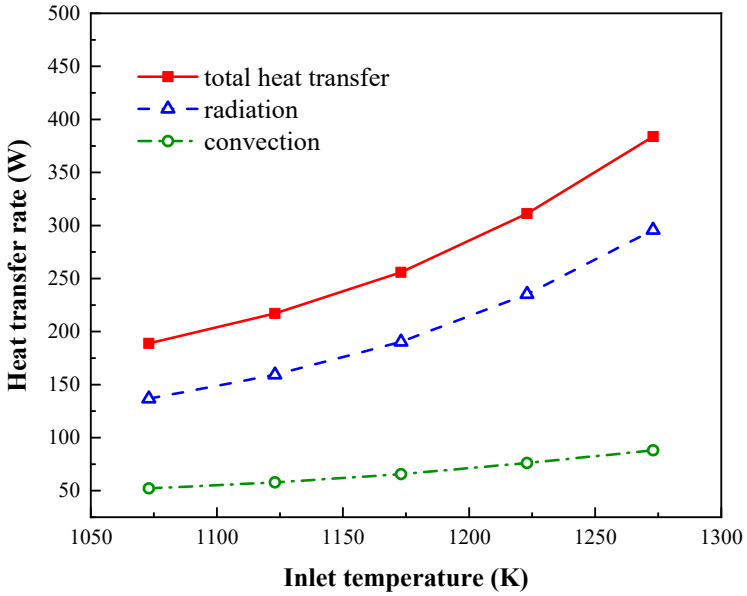


Figure 6. Effect of inlet temperature on heat transfer rate.

4.2. Effects of Sweep Gas Flow Rate

In this section, the effects of the sweep gas flow rate on the performance of the OTMR are analyzed by varying the mass flow rate of sweep gas from 2×10^{-6} to 4×10^{-5} kg/s. The other parameters are fixed at the base case values described in Section 2.3.

The distribution of membrane temperature, the oxygen permeation rate along the axis, and the effect of the sweep gas flow rate on the heat transfer rate are given in Figures 7–9, respectively. It is found that the membrane temperature, the oxygen permeation rate, and the heat transfer rate gradually increase with the increasing sweep gas flow rate. At lower sweep gas flow rate, the change of the membrane temperature and radiative heat transfer rate with the flow rate are less pronounced, while the change of the oxygen permeation rate and the convective heat transfer rate are obvious. This is because at lower flow rate, the content of fuel (i.e., syngas) in the sweep gas is low, leading to a weak combustion reaction, therefore the temperature of the membrane and the sweep gas are both relatively low. Because the membrane temperature changes with a little significance, the change of radiative heat transfer rate is not obvious. However, as the flow rate increases, the sweep gas can take away more unreacted oxygen. Therefore, the oxygen permeation rate has been increasing with the increasing sweep gas flow rate, i.e., a significant increase is achieved even at lower flow rate. In addition, the larger the flow rate, the larger the convective heat transfer coefficient between the gases and the quartz tube wall, therefore the convective heat transfer rate has been increasing with the increasing flow rate, even at lower flow rate. As the sweep gas flow rate increases, the proportion of convective heat transfer is gradually increasing while the proportion of radiative heat transfer is gradually

decreasing. When the sweep gas is supplied at a mass flow rate of 2×10^{-6} kg/s, the total heat transfer rate of 148.73 W is obtained, of which the radiation component is 126.86 W, accounting for about 85%, while the convection component about 15%. Increasing the flow rate to 4×10^{-5} kg/s, the total heat transfer rate increases to 217.59 W, of which the radiation component is 166.13 W, which accounts for 76%, while the convection component increases to about 24%. Therefore, the inlet flow rate of the sweep gas needs to be increased to an appropriate value to enable the combustion reaction to proceed more sufficiently. Increasing the sweep gas flow rate can improve the performance of the membrane reactor. In order to obtain a higher thermal power for the application of the fire tube boiler, the flow rate of sweep gas must be maintained within a reasonable range and should not be too small.

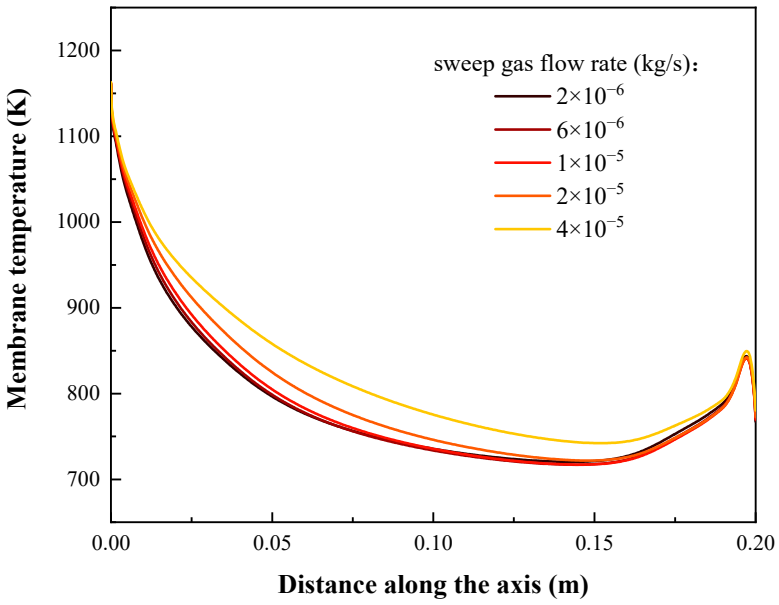


Figure 7. Effect of sweep gas flow rate on membrane temperature distribution.

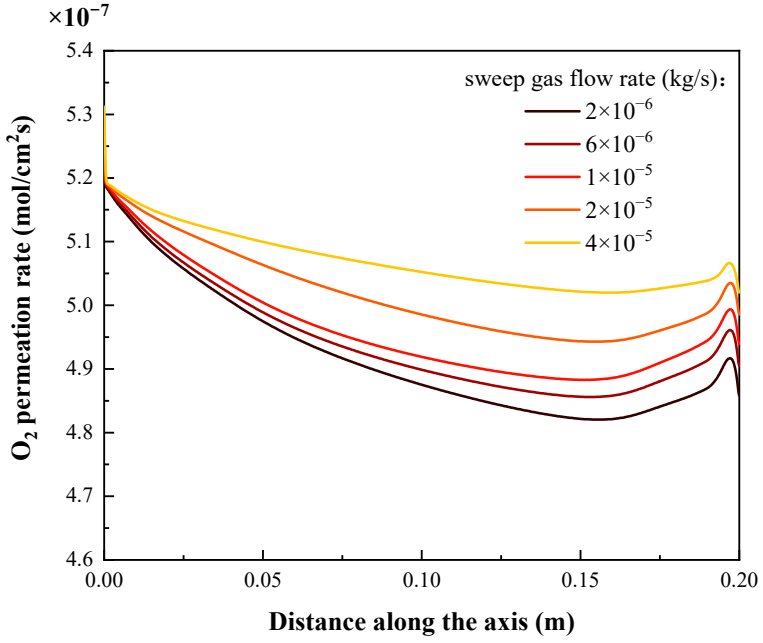


Figure 8. Effect of sweep gas flow rate on oxygen permeation rate.

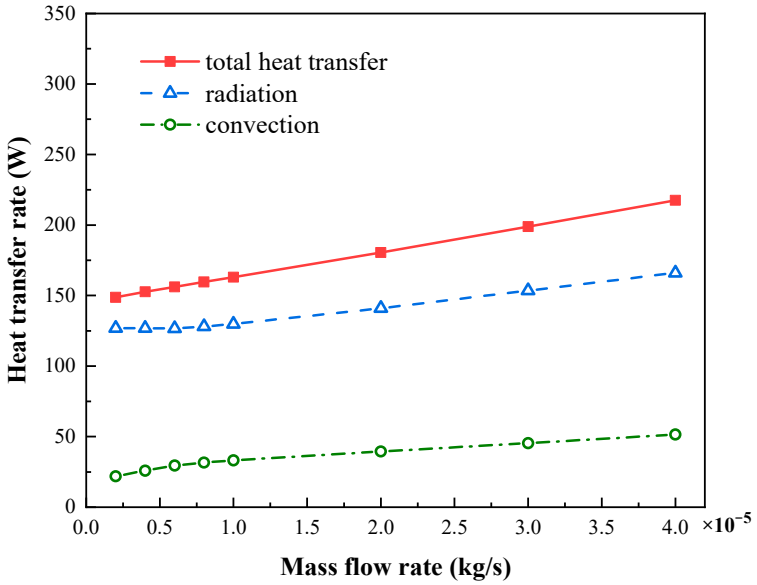


Figure 9. Effect of sweep gas flow rate on heat transfer rate.

4.3. Effects of Syngas Composition

In this section, the effects of the syngas composition, that is, the mass ratio of H_2/CO in the syngas, on the reactor performance for application of the fire tube boiler are investigated. The mass ratio of H_2/CO varies from 0.1:0.9 to 0.9:0.1, while the other parameters are fixed at the base case values described in Section 2.3.

Figure 10 shows the distribution of membrane temperature along the axis under different mass ratios of H_2/CO. It is found that the membrane temperature gradually increases as the H_2/CO mass ratio increases. This is because the enthalpy change of the reaction between O_2 and H_2 per unit mass is much larger than that of the reaction between O_2 and CO per unit mass. For example, at 700 °C, the absolute value of the enthalpy change of H_2 combustion reaction is 123.78 kJ/g, while the enthalpy of CO combustion reaction is 10.10 kJ/g. Therefore, keeping the mass flow rate of the sweep gas unchanged, increasing the H_2/CO mass ratio, that is, increasing the content of H_2 and reducing the content of CO by the same mass, can increase the heat released by the combustion of syngas in the reactor.

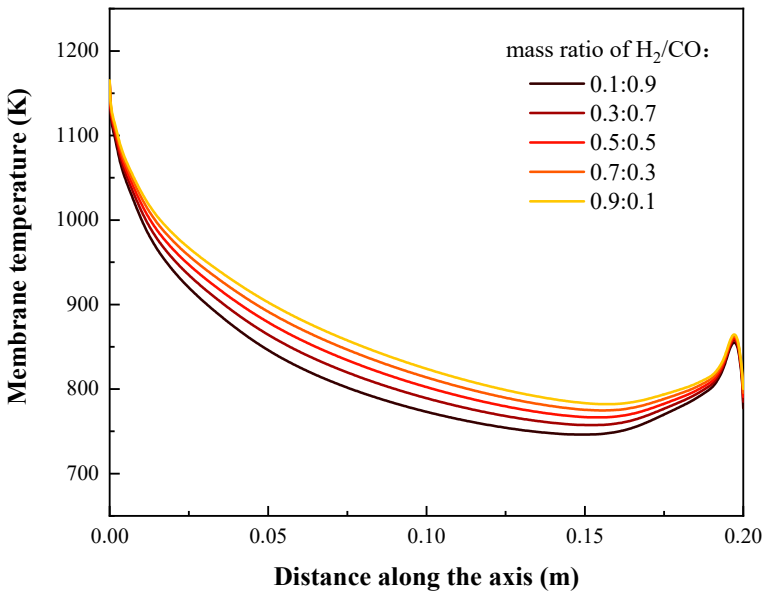


Figure 10. Effect of syngas composition on membrane temperature distribution.

The distribution of oxygen permeation rate along the axis under different H_2/CO mass ratios is presented in Figure 11. Since the membrane temperature increases with the increasing H_2/CO mass ratio, the oxygen permeation rate also increases accordingly. In addition, keeping the mass flow rate of sweep gas unchanged, the volume flow rate of syngas will increase correspondingly when the H_2/CO mass ratio is increased, since the molecular weight of H_2 is smaller than CO. Therefore, the sweep gas will take away more oxygen as the H_2/CO mass ratio increases, and the oxygen permeation rate will also accordingly increase. When the H_2/CO mass ratio increases from 0.1:0.9 to 0.9:0.1, the averaged oxygen permeation rate increases from 4.75×10^{-7} to 5.11×10^{-7} mol/cm^2·s.

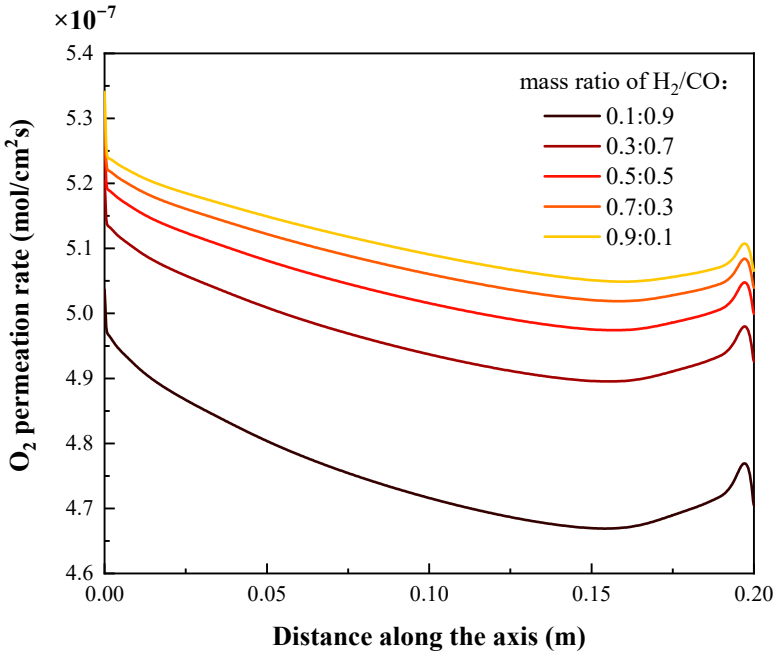


Figure 11. Effect of syngas composition on oxygen permeation rate.

The effect of the H_2/CO mass ratio on the heat transfer rate is shown in Figure 12. It is found that the heat transfer rate gradually increases with the increasing H_2/CO mass ratio, with the proportion of radiative heat transfer decreasing and the opposite trend of convective heat transfer. When the H_2/CO mass ratio increases from 0.1:0.9 to 0.9:0.1, the total heat transfer rate increases from 189.77 to 320.75 W, of which the radiation component increases from 160.66 to 214 W, and the convection component increases from 29.11 to 106.74 W. However, the proportion of radiation drops from 84.66% to 66.72%, while the proportion of convection increases from 15.34% to 33.28%. This is because both the heat released by the combustion of syngas and the membrane temperature increase with the increasing H_2/CO mass ratio, therefore both the radiative and convective heat transfer rates increase accordingly. Moreover, Zheng et al. [25] investigated the infrared radiation characteristics of H_2O and CO_2 gas mixture jet flows at high temperatures of 200–1200 K, and found that in the same infrared band, the more H_2O content in the mixture, the smaller the radiant exitance of the mixture, and the weaker the jet radiation. This explains why, in the present work, since the H_2O content in the product gas increases with the increasing H_2/CO mass ratio, the ratio of the radiative heat transfer to the total heat transfer gradually decreases as the H_2/CO mass ratio increases.

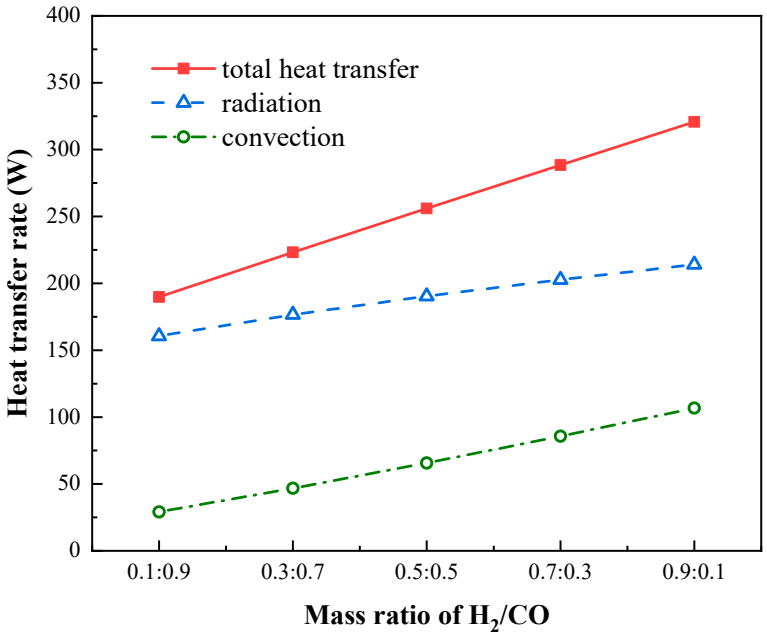


Figure 12. Effect of syngas composition on heat transfer rate.

5. Conclusions

A two-dimensional axisymmetric steady-state CFD model was developed for the syngas combustion in an oxygen transport membrane reactor for application of a fire tube boiler. Effects of inlet temperature, sweep gas flow rate, and syngas composition on the performance of membrane reactor were investigated. The inlet temperature has a strong effect on the oxygen permeability of the membrane and the thermal power of the reactor. A 34-times increase of oxygen permeation rate and a doubled thermal power output can be obtained when increasing the inlet temperature from 1073 to 1273 K. At lower sweep gas flow rate, the change of the membrane temperature and radiative heat transfer rate with the flow rate are less pronounced, while the change of the oxygen permeation rate and the convective heat transfer rate are obvious. Increasing the sweep gas flow rate can improve the performance of the membrane reactor. The membrane temperature, oxygen permeation rate, and thermal power of the reactor all increase with the increase of H_2/CO mass ratio in syngas. After successfully modeling a small scale syngas combustion membrane reactor for use in a tube boiler, future work will focus on scaling up the reactor to improve the thermal power output and better designing the geometry to obtain optimum performance.

Author Contributions: Conceptualization, T.Z. and C.C.; methodology, T.Z.; software, T.Z.; validation, T.Z.; investigation, T.Z.; writing—original draft preparation, T.Z.; writing—review and editing, T.Z. and H.Y.; visualization, T.Z.; supervision, H.Y. and C.C. All authors have read and agreed to the published version of the manuscript.

Funding: This research was funded by the National Natural Science Foundation of China, grant number U1832113.

Institutional Review Board Statement: Not applicable.

Informed Consent Statement: Not applicable.

Data Availability Statement: The data that support the findings of this study are available from the corresponding author upon reasonable request.

Conflicts of Interest: The authors declare no conflict of interest.

References

1. Habib, M.A.; Badr, H.M.; Ahmed, S.F.; Ben-Mansour, R.; Mezghani, K.; Imashuku, S.; Jlo, G. A review of recent developments in carbon capture utilizing oxy-fuel combustion in conventional and ion transport membrane systems. *Int. J. Energy Res.* **2011**, *35*, 741–764. [CrossRef]
2. Joshi, M.M.; Lee, S. Integrated gasification combined cycle-A review of IGCC technology. *Energy Sour.* **1996**, *18*, 537–568. [CrossRef]
3. Zabetta, E.C.; Xilpinen, P.; Hupa, M. Kinetic modeling study on the potential of staged combustion in gas turbines for the reduction of nitrogen oxide emissions from biomass IGCC plants. *Energy Fuel* **2000**, *14*, 751–761. [CrossRef]
4. Casleton, K.H.; Breault, R.W.; Richards, G.A. System issues and tradeoffs associated with syngas production and combustion. *Combust. Sci. Technol.* **2008**, *180*, 1013–1052. [CrossRef]
5. Yuan, R.H.; He, Z.; Zhang, Y.; Wang, W.D.; Chen, C.S.; Wu, H.; Zhan, Z.L. Partial oxidation of methane to syngas in a packed bed catalyst membrane reactor. *AIChE J.* **2016**, *62*, 2170–2176. [CrossRef]
6. Nemitallah, M.A. Characteristics of oxygen permeation and partial oxidation of methane in a catalytic membrane reactor for syngas production. *Energy Fuels* **2020**, *34*, 7522–7532. [CrossRef]
7. Parente, M.; Soria, M.; Madeira, L.M. Hydrogen and/or syngas production through combined dry and steam reforming of biogas in a membrane reactor: A thermodynamic study. *Renew. Energy* **2020**, *157*, 1254–1264. [CrossRef]
8. Hu, T.; Liang, W.; Xia, X.; Peng, H.; Jiang, H. Simultaneous production of pure nitrogen and syngas in $BaCe_{0.5}Fe_{0.5}O_{3-\delta}$ membrane reactor. *Catal. Today* **2021**, *364*, 125–131. [CrossRef]
9. Li, C.; He, Z.; Ban, X.; Li, N.; Chen, C.; Zhan, Z. Membrane-based catalytic partial oxidation of ethanol coupled with steam reforming for solid oxide fuel cells. *J. Membr. Sci.* **2021**, *622*, 119032. [CrossRef]
10. Habib, M.A.; Salaudeen, S.A.; Nemitallah, M.A.; Ben-Mansour, R.; Mokheimer, E. Numerical investigation of syngas oxy-combustion inside a LSCF-6428 oxygen transport membrane reactor. *Energy* **2016**, *96*, 654–665. [CrossRef]
11. Habib, M.A.; Nemitallah, M.A. Design of an ion transport membrane reactor for application in fire tube boilers. *Energy* **2015**, *81*, 787–801. [CrossRef]
12. Ben-Mansour, R.; Adebiyi, A.A.; Habib, M.A. Investigation of performance of fire-tube boilers integrated with ion transport membrane for oxy-fuel combustion. *Int. J. Energy Res.* **2016**, *40*, 1673–1687. [CrossRef]
13. Mansir, I.B.; Ben-Mansour, R.; Habib, M.A. Oxy-fuel combustion in a two-pass oxygen transport reactor for fire tube boiler application. *Appl. Energy* **2018**, *229*, 828–840. [CrossRef]
14. Mansir, I.B.; Ben-Mansour, R.; Habib, M.A. Numerical modeling of heat transfer characteristics in a two-pass oxygen transport reactor for fire tube boilers under oxy-fuel combustion. *Appl. Therm. Eng.* **2021**, *195*, 117248. [CrossRef]
15. Coltrin, M.E.; Glarborg, P. *Chemically Reacting Flow: Theory and Practice*; Wiley-Interscience: New York, NY, USA, 2003.
16. Fluent, I. FLUENT 6.3 user's guide. In *Fluent Documentation*; Fluent Inc.: Lebanon, NH, USA, 2006.
17. McGee, H.A. *Molecular Engineering*; McGraw-Hill: New York, NY, USA, 1991.
18. Xu, S.J.; Thomson, W.J. Oxygen permeation rates through ion-conducting perovskite membranes. *Chem. Eng. Sci.* **1999**, *54*, 3839–3850. [CrossRef]
19. Rui, Z.B.; Zhang, K.; Li, Y.; Lin, Y. Simulation of methane conversion to syngas in a membrane reactor: Part I A model including product oxidation. *Int. J. Hydrogen Energy* **2008**, *33*, 2246–2253. [CrossRef]
20. Cuoci, A.; Frassoldati, A.; Faravelli, T.; Ranzi, E. Accuracy and flexibility of simplified kinetic models for CFD applications. *Combust. Colloq.* **2009**, 1–6. Available online: https://www.researchgate.net/publication/266176558_Accuracy_and_Flexibility_of_Simplified_Kinetic_Models_for_CFD_applications (accessed on 8 July 2021).
21. Nemitallah, M.A.; Habib, M.A.; Salaudeen, S.A.; Mansir, I. Hydrogen production, oxygen separation and syngas oxy-combustion inside a water splitting membrane reactor. *Renew. Energy* **2017**, *113*, 221–234. [CrossRef]
22. Jin, W.Q.; Li, S.G.; Huang, P.; Xu, N.P.; Shi, J.; Lin, Y.S. Tubular lanthanum cobaltite perovskite-type membrane reactors for partial oxidation of methane to syngas. *J. Membr. Sci.* **2000**, *166*, 13–22. [CrossRef]
23. Jin, W.Q.; Gu, X.; Li, S.G.; Huang, P.; Xu, N.P.; Shi, J. Experimental and simulation study on a catalyst packed tubular dense membrane reactor for partial oxidation of methane to syngas. *Chem. Eng. Sci.* **2000**, *55*, 2617–2625. [CrossRef]
24. Barlow, R.S.; Fiechtner, G.J.; Carter, D.C. Experiments on the scalar structure of turbulent CO/H2/N2 jet flames. *Combust. Flame* **2000**, *120*, 549–569. [CrossRef]
25. Zheng, H.J.; Bai, T.; Wang, Q.; Cao, F. Infrared radiation characteristics of high-temperature H2O and CO2 gas mixture jet flows. *Acta Opt. Sin.* **2017**, *37*, 262–272.